NAA-SR-5584
REACTORS-GENERAL
34 PAGES

HALLAM CRITICAL EXPERIMENT

By

R. J. DOYAS

Work Performed By

R. J. DOYAS
C. A. GUDERJAHN
M. S. MAYER

ATOMICS INTERNATIONAL

A DIVISION OF NORTH AMERICAN AVIATION, INC.
P.O. BOX 309 CANOGA PARK, CALIFORNIA

CONTRACT: AT(11-1)-GEN-8
ISSUED:

MAY 1 1961

DISTRIBUTION

This report has been distributed according to the category "Reactors-General" as given in "Standard Distribution Lists for Unclassified Scientific and Technical Reports" TID-4500 (15th Ed.). August 1, 1959. A total of 625 copies was printed.

DISCLAIMER

CONTENTS

	Page
Abstract	v
I. Introduction	1
A. The HNPF Reactor	1
B. The SGR Critical Facility	3
1. General	3
2. Core	3
3. Moderator	4
4. Startup Source	4
5. Control System	5
II. Experimental	6
A. Fuel Elements	6
B. Graphite	7
C. Lattices	9
D. Control Rods	11
III. Experimental Procedures and Results	13
A. Critical Mass	13
B. Fuel-Element Worth	14
C. Graphite-Plug Worths	16
D. Control-Rod Worths	17
1. SGR Control Rods	17
2. HNPF Control Rods	18
3. Single HNPF Control Slug	20
E. Flux Distributions	21
1. Gross Axial and Radial Distributions	21
2. Perturbation of Power Distribution	24
F. Thermal Utilization	25
IV. Calculations	28
A. Methods Used	28
B. Cases Studied: Cell Models	29
C. Results and Comparison	31
1. Buckling	31
2. Critical Mass	31
3. Element Worth	32
4. Fluxes	33
References	34

TABLES

		Page
I.	HNPF Control Elements	11
II.	Critical Loadings	13
III.	Fuel Element Worths	15
IV.	Worth of Fuel in Poisoned-Core-and-Reflector Open Lattice	16
V.	Graphite Plug Measurements	17
VI.	HNPF Control Rod Results	19
VII.	Measurements on a Single Control Element	21
VIII.	Summary of Material Data	28
IX.	Calculated Reflector Savings and Material Bucklings	31
X.	Calculated and Measured Critical Masses	32

FIGURES

1.	SGR Critical Assembly	2
2.	HNPF Critical Fuel Element (112559 7508-5188A)	6
3.	HNPF Critical Core Assembly and Fuel Element	7
4.	Fuel Element Dimensions	8
5.	Open Lattice - 16 Elements	10
6.	Full Lattice - 17 Elements	10
7.	Open, Poisoned Lattice	10
8.	Full, Poisoned Lattice - 26 Elements	10
9.	Experimental HNPF Control Element	11
10.	Calibration Curve of Control Rod No. 4	18
11.	Calibration Curve of Rare-Earth Control Rod	20
12.	Radial Thermal Flux Distribution	22
13.	Axial Flux, Traverse Along Poison Holder	23
14.	Radial Flux, 30-Element Lattice	23
15.	Axial Flux, 30-Element Lattice	24
16.	Power Distribution in a Perturbed Fuel Element	25
17.	Calculated Radial Fluxes in Open, Poisoned Lattice	33

ABSTRACT

This report presents the results of a critical-experiment program conducted to study the Hallam Nuclear Power Facility (HNPF) reactor concept and to verify design parameters. Experimental procedures and results are given, and comparisons are made with calculational techniques currently in use for determining the nuclear characteristics of the HNPF reactor.

I. INTRODUCTION

A series of critical experiments using fuel similar to that planned for the HNPF has been performed at the Sodium Graphite Reactor (SGR) Critical Facility to assist in the final design of the HNPF reactor. Measurements of certain criticality parameters and the reactivity worths of several types of control-rods have been made for several kinds of lattices. The purpose of making these measurements was to give aid in setting the final fuel enrichment value and in defining the control requirements. Also studied were reactivity worths of several different fuel elements, including a second-loading uranium-carbide element. Core flux distributions were measured, and a study was made of the perturbation of the local power distribution caused by a partially inserted control rod.

Calculations were made on the various lattices, both as an aid in planning the experiments and for comparison of present analytical techniques with experimental results. These experiments were performed in conjunction with a series of exponential experiments which used the same fuel elements and determined the intensive nuclear parameters for a series of lattice spacings; therefore little intracell work was required to be done in the critical assembly. The results of the exponential work will be forthcoming in a separate report.[1]

Application of the results of the critical experiments to the design of the HNPF is not covered in this report.

A. THE HNPF REACTOR

The Hallam Nuclear Power Facility, currently under construction at a site near Hallam, Nebraska for the United States Atomic Energy Commission, is designed to generate a steady-state power of 256 Mw thermal, 75 Mw electrical. The plant will be operated by the Consumer's Public Power District of Nebraska; the power will be fed into the existing power distribution network. The reactor is graphite-moderated, sodium-cooled, and fueled with uranium - 10 wt% molybdenum alloy, enriched to 3.6 wt% U^{235}.

The moderator will be in the form of stainless-steel-clad hexagonal graphite logs, 16-in. across flats with corners scalloped for fuel locations. The sodium coolant is pumped upward, around and through the element, and between adjacent graphite logs.

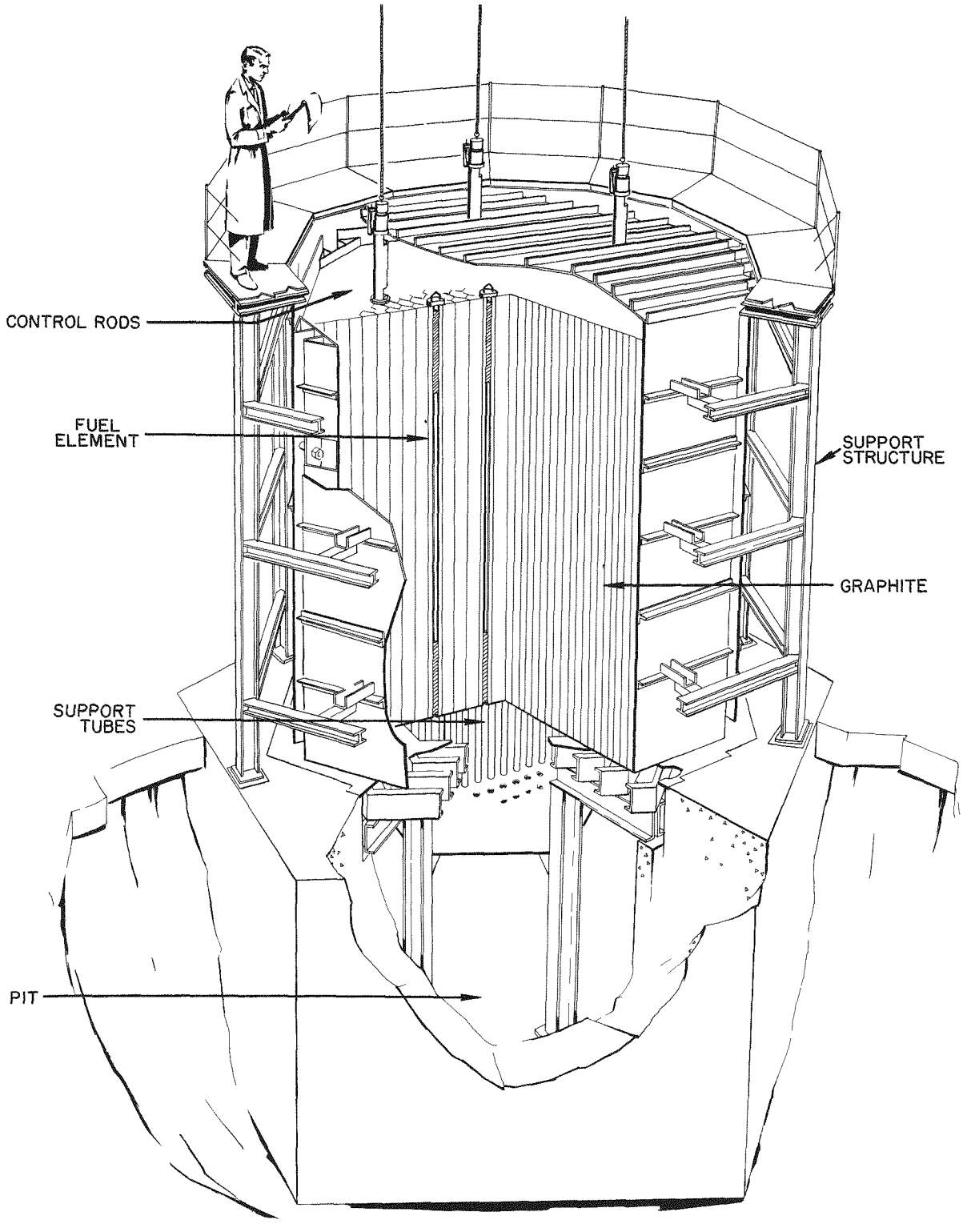

Figure 1. SGR Critical Assembly

The fuel element is composed of 18 U-Mo rods arranged in a cluster about a center tube of stainless steel; the planned second-core loading will use uranium carbide fuel rods. The rods are surrounded with a NaK bond and individually clad in stainless steel, and the cluster is enclosed in an open-end Zircalloy process tube. The control-safety rods will be located in fuel-element channels, replacing every sixth fuel element in the central core region. The control rods will be an equal mixture of Gd_2O_3 and Sm_2O_3, with an active length of 12.5 ft., and will operate in helium-filled thimbles. The first core loading will consist of 137 fuel elements, 10 of which may be UC; the remainder will be U-Mo, with 19 driven control safety rods, six fixed control rods which replace additional fuel elements near the center of the core, and 39 graphite dummy elements at the outer edge of the core.

The active core will be 13.5-ft high by 12.9-ft diameter; the total core is 17-ft high by 16.8-ft diameter. The average at-power temperatures of the sodium, fuel, and graphite are all in the range 400-450°C. The initial unpoisoned k_{eff} of 1.100 is designed to allow 2.0% Δk for control and xenon, 3.8% Δk for fixed control rods, and about 4% Δk for the initial burnup period. A more detailed description of the HNPF is available in Reference 2.

B. THE SGR CRITICAL FACILITY

1. General

These experiments were performed on the SGR Critical Assembly (Figure 1) which is described more fully in the Hazards Summary.[3] This assembly has been designed to permit experiments on graphite-moderated reactors of various sizes and fuel-element configurations. It consists of a cylindrical array of hexagonal graphite logs into which fuel and poison elements may be placed in a wide variety of lattice spacings and arrangements. Provision is made for air heating the assembly in order to study temperature effects. Features of the facility, pertinent to the interpretation of the experiments, are given below.

2. Core

The graphite forming the basic array is contained in and supported by a nominal "tank" made up of flat mild-steel plates, 1/4-in. thick. The twelve sides of the core "vessel", used to approximate a cylinder, are supported by a ring of beams arranged around the tank in such a manner that they can be

adjusted laterally and tightened, once the moderator logs are loaded inside. This design permits study of reactors of various diameters. The height of the reactor also may be easily adjusted by addition of another layer of graphite logs, structural supports, and side plates. Reactors from 10 to 14 ft in diameter and up to 17 ft in height can be accommodated, by slight modifications of the basic structure. The initial size of the core tank was 12 ft in diameter and 13 ft high. The bottom of the tank is made of 1/4-in.-thick mild-steel plate supported by 10-in. channel beams. The bottom has a hexagonal opening in the center of the vessel which is 6 ft 3-1/2 in. across the flats. Graphite moderator logs in this area are individually supported on 3-1/2-in. diameter steel tubes. The bottoms of the tubes rest on a 2-1/2-in-thick steel plate located 2-1/2 ft below the hexagonal opening. A platform encircles the tank at approximately the same elevation as the top of the core vessel to enable personnel to work on the reactor.

3. Moderator

The moderator consists of hexagonal graphite logs 4 in. across the flats and 4 ft long. The assembly consists of two layers of these logs standing on end, with 1171 logs in each layer. Individual graphite logs may be removed from the core by pushing them from below, with a jack, through holes in the bottom plates which support the logs. Special graphite logs which have a milled slot on two adjoining edges are used at the points where control rods are inserted. The control rods travel vertically in the 1/4-in.-wide x 2-in.-long slots formed by three adjacent control-rod logs. Three logs which have been milled out on a 2.386 in. radius, about a corner, are faced toward a common center to provide a fuel element location. Round plugs of 4.74-in. diameter are used both as end plugs on the fuel elements and for filling vacant fuel locations.

4. Startup Source

The startup source for the reactor is a polonium-beryllium neutron source with a strength of 2×10^7 n/sec. It is located in a vertical hole drilled into one of the graphite logs, and is attached to a drive similar to that used for the control rods for removal from the core after criticality is attained. The source is contained in a 20-ft-long, aluminum-clad, graphite rod, so that its removal does not leave a void, and moderator continuity is only slightly perturbed at all times.

5. Control System

Poison elements which are combination shim, regulating, and safety elements are used to control the critical assembly. The number of elements and their positions in the assembly can be varied as required by the experiments being performed. Nine control rods were used for all of the Hallam lattices.

The poison element is composed of three V-shaped 0.032-in.-thick plates of a 70% silver - 30% cadmium alloy, joined in the shape of a "Y" with 1-7/8-in. arms. The poison elements move vertically in slots milled from the surfaces of three graphite moderator logs at the intersection of the logs. A steel tube, mounted on top of the graphite, contains two sets of rollers which guide the poison element. This tube also contains a lower-limit microswitch and a lead-shot snubber.

The rod drive units are located in the penthouse directly over the critical cell. The units are modified aircraft-autopilot servo motors, each with a drum on which the cable supporting the control rods is wound. The rod drive units are fail-safe since interruption of brake solenoid power results in a scram.

Figure 2. HNPF Critical Fuel Element

II. EXPERIMENTAL

A. FUEL ELEMENTS

Fuel elements mocking up the HNPF fuel design were used. A typical fuel element (Figures 2, 3, and 4) consisted of a 66-in.-long, 4.74-in.-diameter, aluminum cylinder containing 19, 0.604-in.-diameter holes to receive 18 fuel-slug columns (the center hole was left empty to conform to a late HNPF design change). The fuel pins are solid bare rods, 0.592-in.-diameter, 3.448 at.% enriched uranium metal alloyed with 10 wt % molybdenum. The aluminum in the elements served as a mockup for sodium coolant. No material equivalent to the stainless steel fuel cladding and the process tube of the HNPF fuel element was included.

The elements were hung from the top of the reactor by hanger rods supported by the graphite surface. Graphite end plugs filled the channel as shown in Figure 4, thus completing the axial reflectors. A 2-1/2-ft void below the fuel elements allowed them to drop partly out of the core in the event of an accidental melt-down.

Besides this basic element, single mockups of several other fuel elements were available for study: a 19-rod element (from the previous fuel design), a reduced-enrichment (2.778 at.%) U-Mo 18-rod element, and a 12-rod 3.448 at.% enriched uranium carbide element.

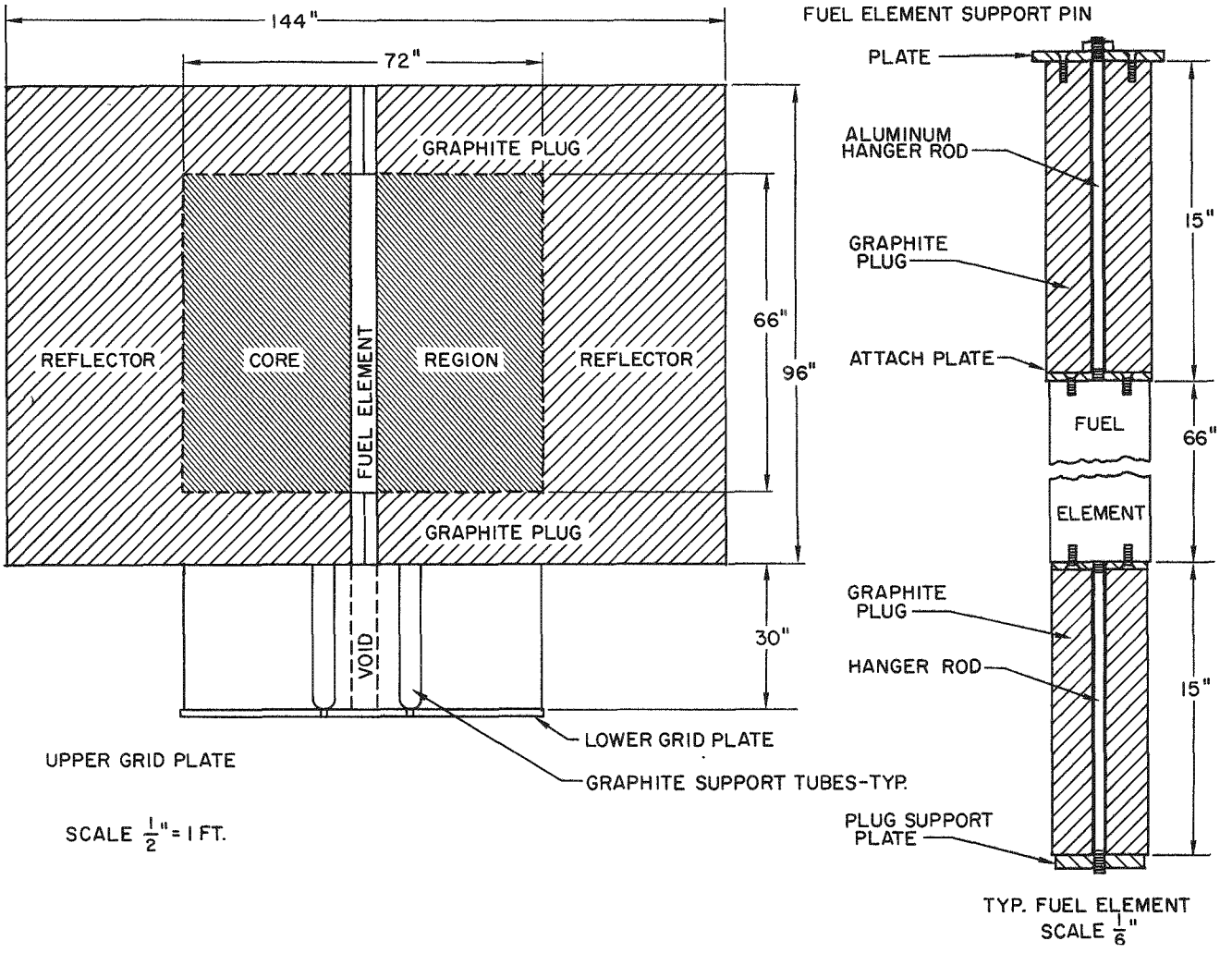

Figure 3. HNPF Critical Core Assembly and Fuel Element

B. GRAPHITE

Sigma-pile experiments on a solid column of SGR graphite 8 ft high x 12 ft in diameter, using a PoBe neutron source placed 2 ft from the bottom of the pile, gave the following values for the graphite constants:

$$L^2 = 2381 \text{ cm}^2$$

$$D = 0.872 \text{ cm}$$

$$\Sigma_a = 0.000366 \text{ cm}^{-1}.$$

Where $\rho = 1.67$ gm/cc

and $T = 20°C.$

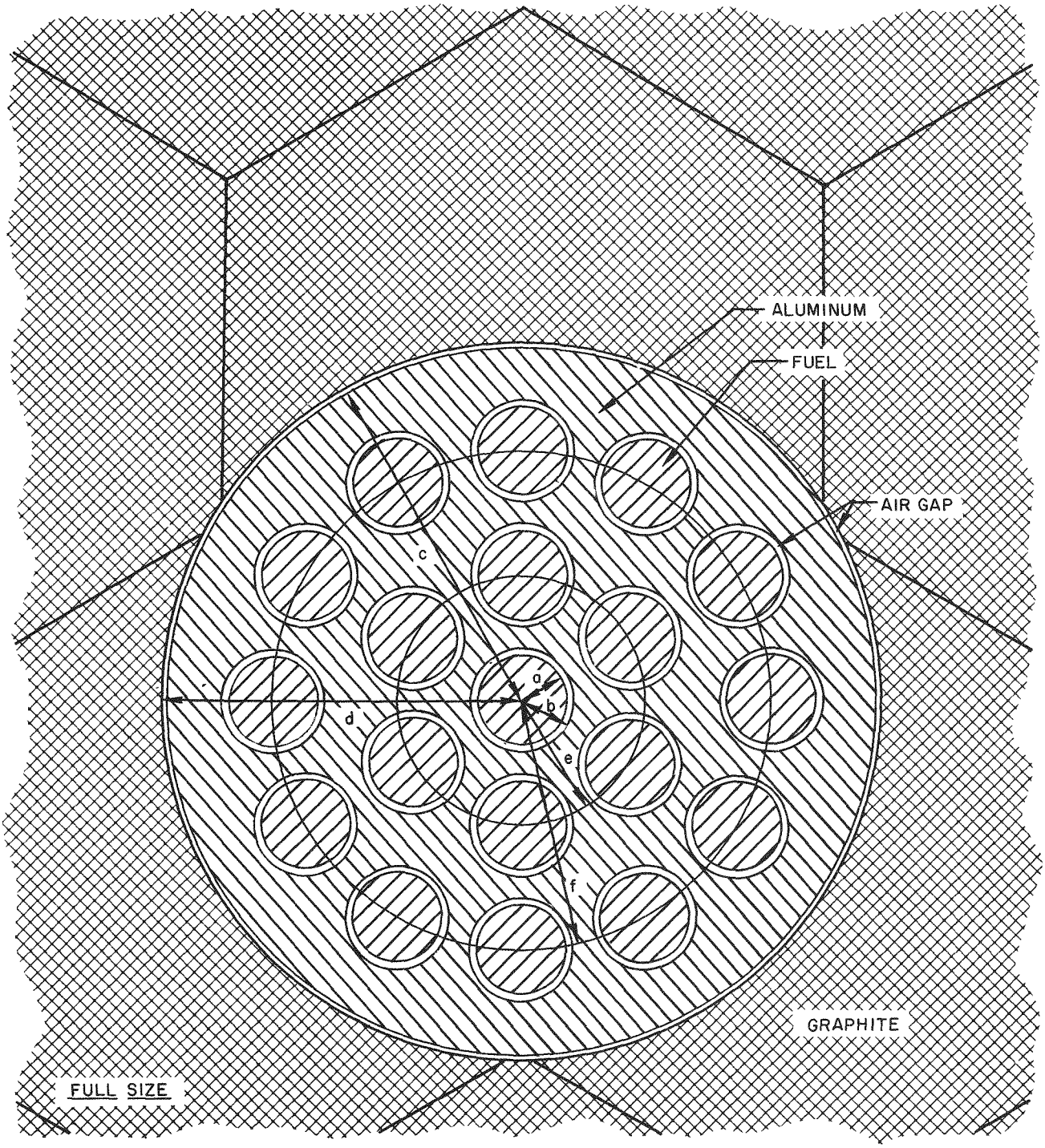

Fuel: U 3.448 a/o Enriched, 10.15 w/o Mo

Density of Fuel	17.12 gm/cm^3	c = 2.370 in. Radius	
Density of Graphite	1.68 gm/cm^3	d = 2.386 in. Radius	d-c = 0.16 in. R, 0.032 in. Dia.
Density of Aluminum	2.71 gm/cm^3		
a = 0.296 in. Radius	Air Gap	e = 0.872 in. Radius	
b = 0.302 in. Radius	b-a = 0.006 in. R, 0.012 in. Dia.	f = 1.660 in. Radius	

Figure 4. Fuel Element Dimensions

The graphite to be used in the HNPF will be quite different: mold-type graphite is specified, for which the following values[4] are assumed in making intercomparisons:

$$L^2 = 2068 \text{ cm}^2$$

$$D = 0.872 \text{ cm}$$

$$\Sigma_a = 0.000422 \text{ cm}^{-1}.$$

No attempt was made to mock up the cladding of the HNPF graphite logs.

C. LATTICES

The lattices studied in this experiment has a slightly different lattice spacing from the HNPF lattice; i.e., the center-to-center fuel element distance was 9.228 in. as compared to 9.237 in. for the HNPF lattice. This difference was due to the geometry of the SGR graphite logs. The fuel elements were 66 in. long (see Section II-A), and the graphite was 8 ft high; therefore, the 5-1/2-ft-high core was reflected axially by 1.25 ft of graphite.

Two main types of lattices were constructed: an "open" lattice (five fuel locations plus one void location per hexagonal cell) and a "full" lattice (fuel at all six locations of the cell), Figures 5 and 6. The open lattice was also studied with graphite filling the void sites in order to achieve a simpler case with which to compare calculational methods.

Because of the small number of elements needed to achieve criticality in these lattices, there were few repeating cells, particularly in the open lattices, and reflector effects were large. In order to increase substantially the core diameter of the lattices, the core was poisoned by introducing stainless steel tubes to approximate the neutron absorption of the moderator cans in the HNPF reactor. These type 304 stainless steeltubes were 1.9 in. OD, 65-mil wall thickness, and 8 ft long. They were placed throughout the core in the centers of hexagonal rings of fuel, as shown in Figures 7 and 8. The lattices thus formed are referred to as the "open-poisoned" and "full-poisoned" lattices. In one case, the poison was also introduced into the reflector of the open poisoned lattice, forming a region of poisoned radial reflector.

Moderator logs with a 2-in.-diameter hole were located throughout the core in these lattices, and filled with graphite plugs. These holes provided foil holder locations for use in making flux traverses.

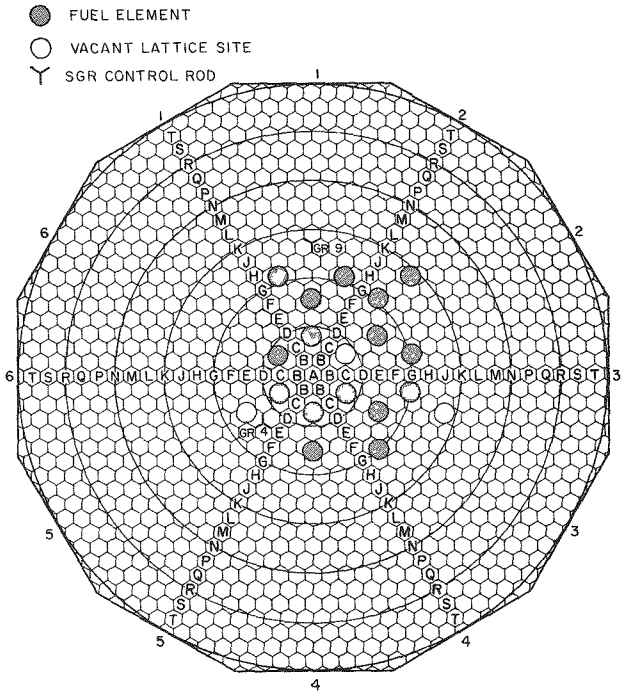

Figure 5. Open Lattice–
16 Elements

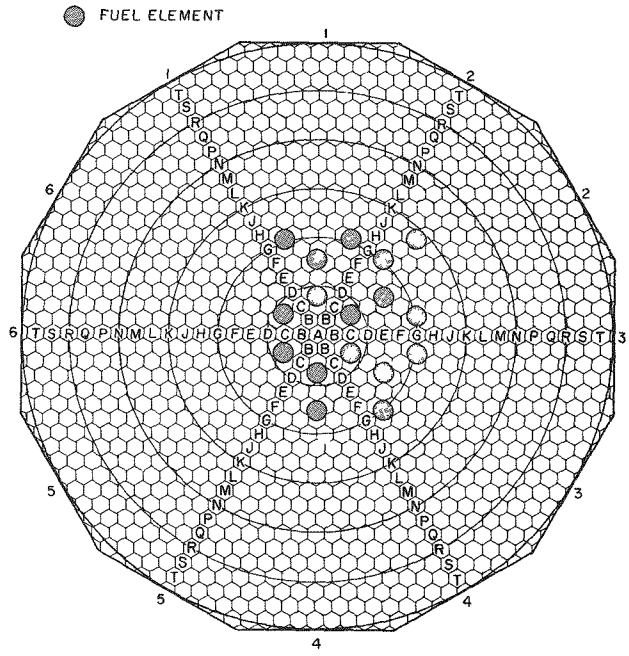

Figure 6. Full Lattice–
17 Elements

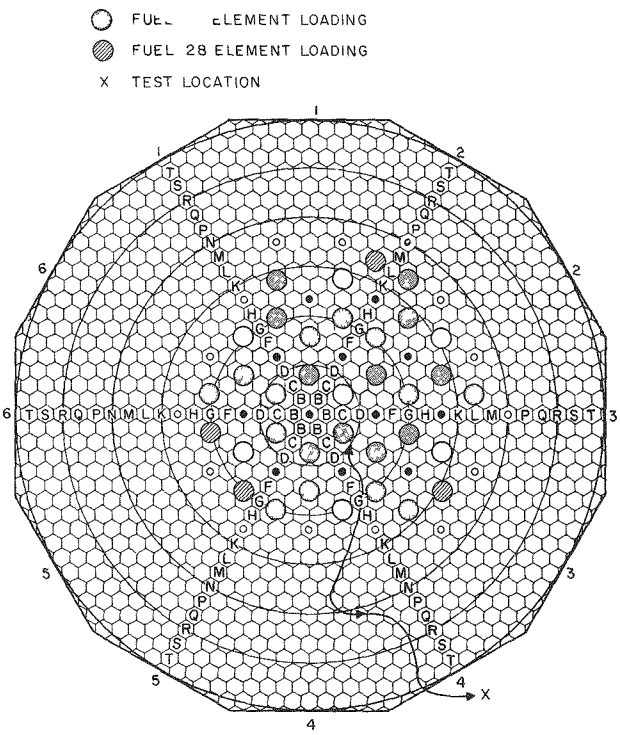

Figure 7. Open, Poisoned Lattice

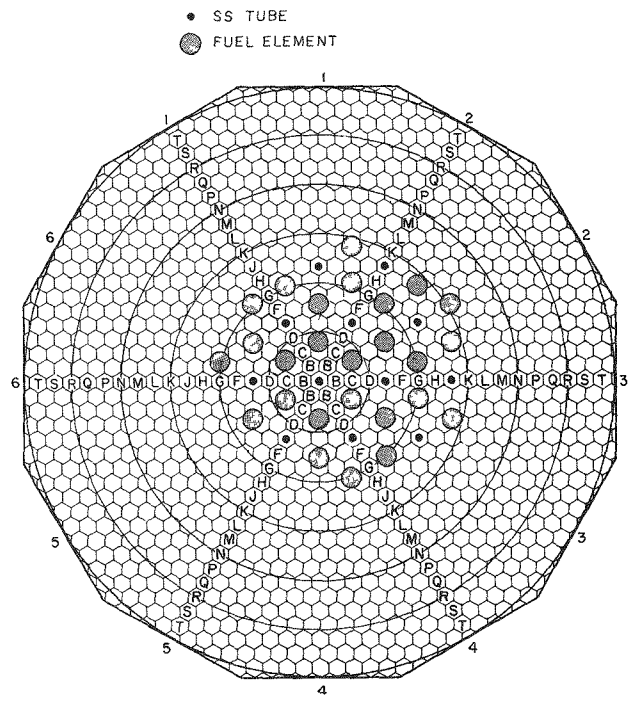

Figure 8. Full, Poisoned Lattice–
26 Elements

D. CONTROL RODS

Mockups of several control-rod designs were available for intercomparisons and for determination of absolute values of control-rod worths. Some of these are shown in Figure 9, along with the holders used in the experiments. The

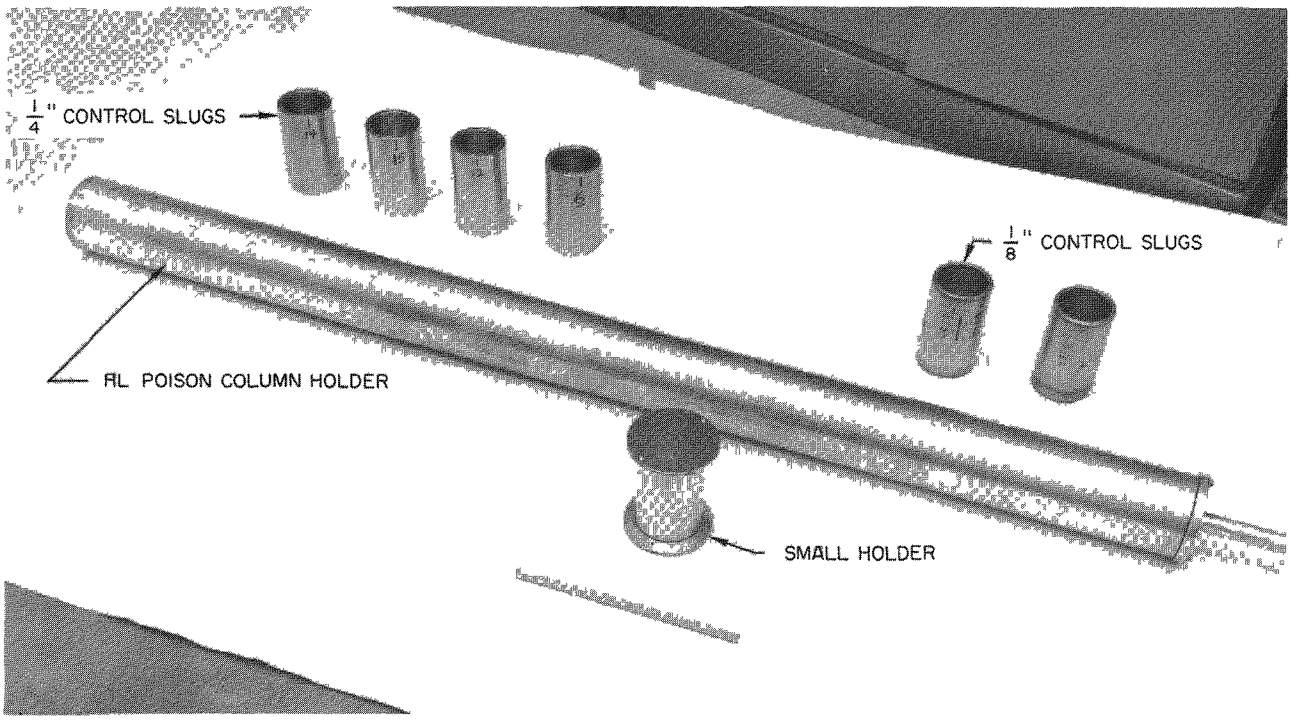

Figure 9. Experimental HNPF Control Element

large holder was 5.5 ft long, 1/2 in. thick, and was made of type-1100 aluminum; a 0.096-in.-thick zirconium sheath could be inserted over this to simulate the Zircalloy process tube of the HNPF control-rod thimble. The poison elements were 6-in.-long steel cylinders, 3-3/8-in.-OD, in which were compacted various mixtures and thicknesses of rare earth oxides, as detailed in Table I.

TABLE I

HNPF CONTROL ELEMENTS

Material	Thickness (in.)	Density (gm/cm^3)	Pack Weight (g)
Rare-earth (45-45%)	1/4	5.46	1268.9
Rare-earth (45-45%)	1/8	5.46	755.3
B_4C	1/4	1.63	354.8
90% Gd_2O_3	1/8	4.76	652.8

A small thin-walled aluminum holder for single-slug experiments, also shown in figure 9, was available; a 20-mil cadmium cylinder and end-plates could be inserted around the poison slug being studied in this holder to separate epicadmium and total reactivity worths.

III. EXPERIMENTAL PROCEDURES AND RESULTS

A. CRITICAL MASS

The critical mass was determined for the various lattices by loading the core radially in steps involving integral numbers of elements. Near criticality, the steps consisted only of single elements. The excess reactivities of the critical loadings were measured using the rod-calibration technique discussed in section III-D-1. The results of these measurements are shown in Table II for the various lattices

TABLE II

CRITICAL LOADINGS

Lattice Type	Figure	No. of Holes Voided*	No. of Elements	Excess ρ, (cents)
Open	5	4	17	94.2
Open	5	0	16	92.1
Full	6	-	17	23.3
Full, poisoned	8	-	26	44.5
Open, poisoned	7	0	25	202.8
Open, poisoned Core and reflector	7	0	28	27.6
Open, poisoned Core and reflector		1†	29	46.5

*The unoccupied lattice sites in the open lattice (every 6th fuel element location) were plugged with graphite for the critical mass determinations except as noted here. No vacancies exist in the full lattices.
†Central.

The lattices were centered not about the center of the SGR critical facility core, but rather about one of the fuel sites removed 9.24 in. from the center of the core. This permitted control-rod worth measurements and danger-coefficient experiments to be performed at the center of the lattice, thereby avoiding the necessity of applying buckling corrections to the results. Since

the reflector thickness was, in all cases, more than two feet, and usually three feet (effectively infinite), the variation of the reflector thickness over an azimuthal angle had little effect on these measurements.

The critical diameters of the various lattices were only about four to five feet, as may be seen in Figures 5-8. With such small cores and thick reflectors, direct, accurate measurement of the geometrical bucklings would be difficult because of the smallness of the region of asymptotic flux. Moreover, the number of repeating cells was very small, and readily available foil locations were limited to relatively large separations.

B. FUEL-ELEMENT WORTHS

Following the reactivity determinations of the critical lattices, various experiments were performed to determine other data such as peripheral and central element worths. These were measured by making the desired substitution in the core, again finding the total excess reactivity of the lattice, then equating the net reactivity change to the difference between this measurement and the reference reactivity.

In the determination of the central-element worth in the full lattice, measurements were made both with and without the graphite end plugs on the element. When the plugs were removed, the element's worth was slightly negative with respect to a void at that location. This result had been somewhat anticipated from the results of theoretical calculations, since the calculated material buckling of the full lattice was smaller than that for the open lattice; however, a streaming correction had not been applied to the voids in the open lattice calculation, and the actual streaming effects could have nullified this result had they been much larger.

A summary of these measurements is given in Table III. All reactivity worths given in this report are with respect to a void unless specifically noted otherwise. The shadowing interaction between control rods and this effect on the results has not been determined; hence, error limits are not assigned to the tabulated measurements, although the individual period and reactivity determinations are generally accurate to ±0.2 ¢, and rod positioning error is ±1 mm, corresponding to ± <0.2 ¢/step in all cases. Various small reactivity effects, such as temperature changes, control-rod voids, voids in the plugs for hanger rods, hanger rods, nonuniformities, and air pressure, were not taken into account

TABLE III

FUEL ELEMENT WORTHS

Lattice	Location	Total No. of Elements	Worth Relative to Void (cents)
Open	Peripheral	17	+ 103.7 (symmetric location)*
			+ 123.4 (tight location)*
	Peripheral	18	+ 95
	Peripheral	19, 20	+ 83.8†
	Peripheral	21, 22	+ 88.0†
	Peripheral	23, 24	+ 82.4†
Full	Peripheral	18, 19	+ 108.0†
Open, poisoned core and reflector	Peripheral	29	+ 80.3
	Central§	29	+ 23.1
Full	Central	19	+ 5.5
	Central	17	+ 3.4 (symmetric lattice)
	Central	17	+ 0.5 (tight lattice)
	Central (end plugs removed)	17	- 17.2 (tight lattice)
	Central (U-Carbide)	17	+ 61.8
Full, poisoned	Peripheral	26	+ 38.7** (tight location)
Full, poisoned	Peripheral	27	+ 57.2** (symmetric location)

*"Tight location" refers to a peripheral element located in a non-symmetric lattice position relative to the center of the core, in which it has more neithboring elements.
†Measured in pairs only.
§This location is a vacancy for this lattice, and corresponds to a full lattice site.
**With respect to a graphite plug.

since these effects were negligible. The reference in the table to "symmetric" and "tight" locations differentiates the positioning of a peripheral element in its correct location, where it is symmetrically located with respect to the center of the lattice and projects considerably into the radial reflector because of the small core diameter, and in a non-symmetric location, in which it has more neighboring elements. The large additions of fuel in the open lattice were made in the course of the control-rod measurements (Section III-D-2).

The worths of several different fuel designs were measured in the 29-element poisoned-core-and-reflector open lattice, in a test location just off center (Figure 7). The central location in this lattice corresponded to a control-rod (void) lattice site, but was plugged with graphite for these measurements, as were the other void locations. A summary of these measurements is given in Table IV.

TABLE IV

WORTH OF FUEL IN POISONED-CORE-AND-REFLECTOR OPEN LATTICE
(In the next-to-center location)

Fuel Type	Relative to Graphite (cents)	Relative to Void (cents)
18-rod U-Mo	93.6	119.5
UC	122.7	148.6
19-rod U-Mo	93.8	119.7
2.778 at.%, 18-rod U-Mo	50.9	76.8

C. GRAPHITE-PLUG WORTHS

The effect on reactivity of removal or insertion of graphite plugs in the open lattice sites was noted. These changes could be attributed primarily to loss of neutrons due to streaming (the open lattice is near the minimum of the critical-mass vs fuel-to-moderator-ratio curve) and can thus provide a check on calculated streaming corrections. These measurements are given in Table V; the reactivity shown is the worth of the graphite plug with respect to the resultant void (air) at the location listed.

TABLE V

GRAPHITE PLUG MEASUREMENTS

Lattice	No. Fuel Elements	Material	Location	Worth (cents)
Open	22	3 graphite plugs	3 peripheral void locations	+ 54.2
Open	18	graphite plug	central void	+ 66.5
Open	18	3 graphite plugs	3 peripheral void locations	+ 49.6
Open	16	graphite plug	central void	+ 72.3
Open	18 + poison holder	graphite end plug (1.25 ft)	top of poison holder center hole	+ 7.7
Open, poisoned core and reflector	29	graphite plug	central void	+ 45.7
Open, poisoned core and reflector	29	graphite plug	peripheral void	+ 14.7
Open, poisoned core and reflector	29	graphite plug	just-off-center fuel location	+ 25.9

D. CONTROL-ROD WORTHS

1. SGR Control Rods

Various determinations of control-rod effectiveness were made on SGR control rods, primarily for the purpose of determining the excess reactivities of the various lattice configurations. The procedure followed was to determine the critical position with a single control rod where possible, then reduce power and withdraw this rod a sufficient distance to obtain about a 30-sec period. After sufficient counts were obtained, criticality was reestablished by partial insertion of another control rod, and the process repeated until the original rod was fully withdrawn. The reactivity data were reduced on the IBM 709 using a period code to which an approximate value of ℓ/β was supplied.[5]

For small reactivity changes, previous rod-calibration curves were generally assumed valid, and data were taken only to a known point on the rod.

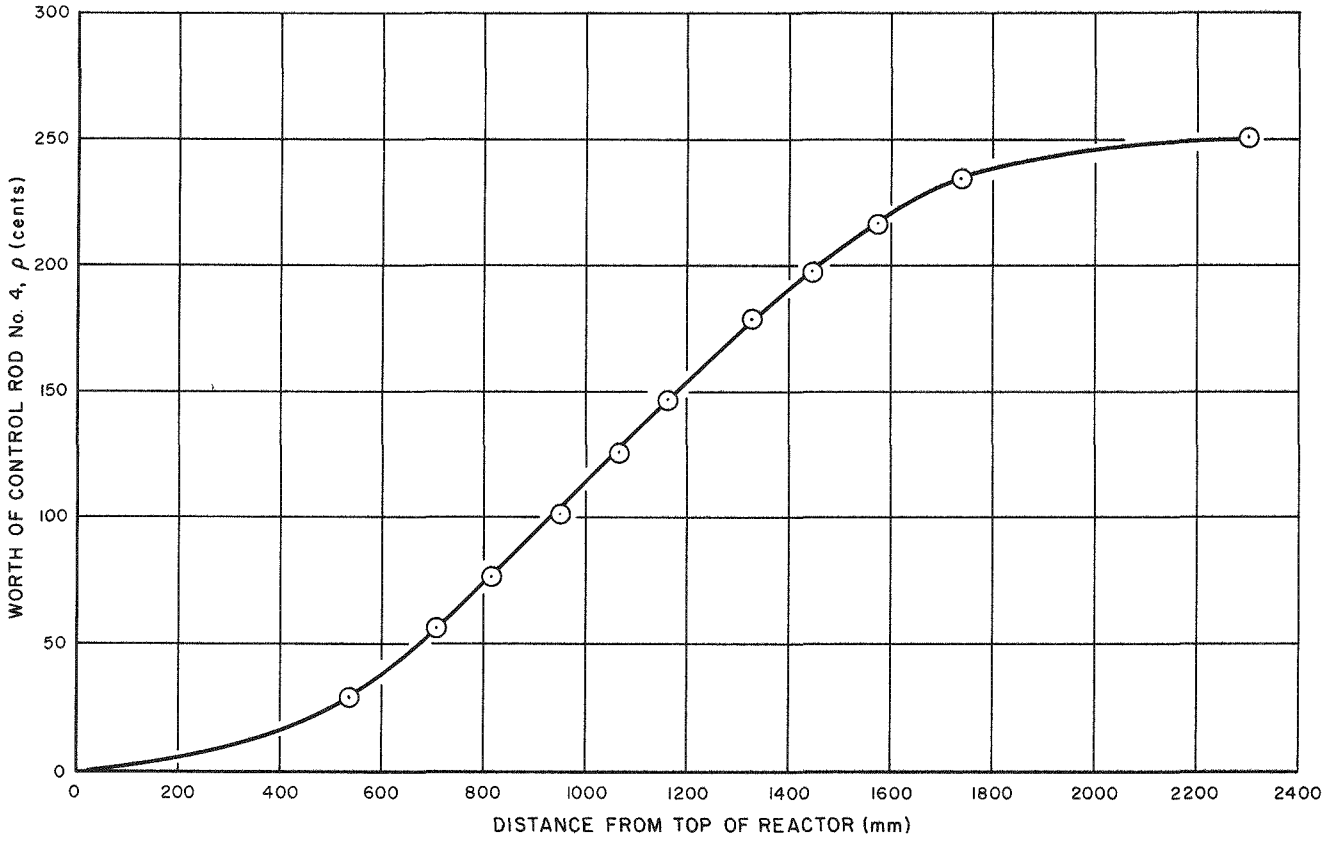

Figure 10. Calibration Curve of Control Rod No. 4

However, for large changes such as the addition of a fuel element, the rod worth changed significantly, and the entire curve had to be redetermined.

The SGR control rod normally used for control and reactivity measurements was rod No. 4 (see Figure 5), with rod No. 9 opposing it for calibration purposes. A typical calibration curve of rod No. 4, taken for the 22-element open lattice, is shown in Figure 10.

2. HNPF Control Rod

The effectiveness of an HNPF-type control element was measured at the central (void) location of the open lattice. The experiment was done in steps; by adding poison slugs, building from the bottom edge of the core; by adding peripheral fuel elements, as necessary; and noting, at each step, the change in reactivity worth from the previously determined rod-calibration curve. Graphite end plugs were positioned on the aluminum poison holder, just as on the fuel elements.

A correction must be applied to the observed reactivities, since the addition of fuel increases the effective core size and thereby reduces the reactivity of any slug inserted into the enlarged core with respect to that which would be measured in the initial core. Since this correction was found not to be very large, the following approximate expression was used to normalize all measured values to the initial 20-element core size (21 cells):

$$\rho_o = \rho_i \frac{(R_i + \delta)^2}{(R_o + \delta)^2}$$

where R_i = core radius = $\sqrt{\frac{\text{no cells x cell area}}{\pi}}$

δ = calculated reflector savings

This kind of correction, among others, must also be applied when extrapolating these worths to the Hallam reactor. No correction was made for possible shadowing effects between the added slugs and rod No. 4, or between rod No. 4 and rod No. 9.

The measured and corrected values are indicated in Table VI, and a plot of the integral and differential data is shown in Figure 11.

TABLE VI

HNPF CONTROL ROD RESULTS

No. Fuel Elements	No. Poison Slugs	ρ (Observed) Rare Earth (cents)	Correction Factor	$\Sigma\rho$ (Corrected) Rare Earth (cents)	$\Sigma\rho$ (Corrected) B_4C (cents)
20	1, 2, & 3	-184.9	1.000	-185	-204
22	4	-78.9	1.07	-269	-
22	5	-93.6	1.07	-370	-403
22	6	-87.7	1.07	-463	-
24	7	-78.8	1.16	-555	-
24	8	-77.7	1.16	-645	-
24	9	-65.5	1.16	-721	-
(extrapolated)	11	-	-	-825	-

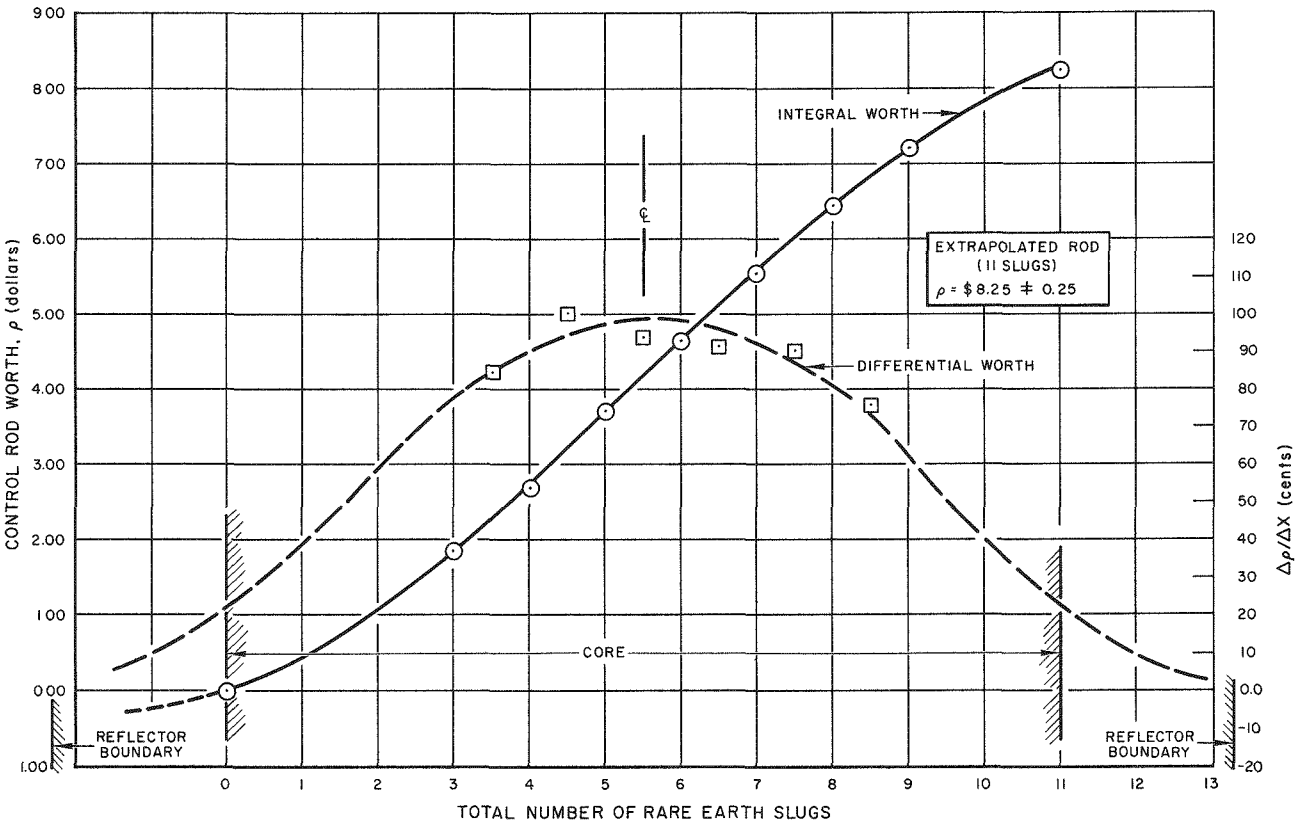

Figure 11. Calibration Curve of Rare-Earth Control Rod

Three B_4C slugs were substituted for the rare-earth slugs at the bottom of the control column when more than six slugs were to be inserted in the rare-earth measurements, and a new reference point was determined from the new critical position. The worths of the two types are so similar, that little error is incurred by doing this. The final total worth value for eleven slugs was found by extrapolating the differential curve and integrating to get the additional worth, in preference to extending the core still further to obtain the necessary reactivity for further measurement.

The worth of the aluminum poison holder was -87.3 cents; that of a zirconium sleeve around the holder was -4.0 cents, when observed with five rare-earth slugs in the poison holder. The sleeve was not in position during the rod-worth experiments.

3. Single HNPF Control Slug

Experiments to study the relative thermal and epithermal worths of the various HNPF poison slugs were performed on single slugs at the center of both

the open and the open poisoned lattices. The results of the measurements, indicated in Table VII, show that there is little difference in control worths among the various elements tested. The procedure was to position the individual slugs in the reactor, with and without a cadmium cover, in the small holder described in section III-D. In each step, the critical position was found, and reactivities were determined from the calibration curve of control rod No. 4 for this loading; the effect of the poison slug on the rod calibration was not considered.

TABLE VII

MEASUREMENTS ON A SINGLE CONTROL ELEMENT
(At the center of the lattice)

Lattice	Poison Control Element Thickness	Composition	Negative Reactivity Worth (cents)		
			Epicad.	Thermal	Total
Open	1/4-in.	Rare earth (45% Gd_2O_3, 45% Sm_2O_3, 10% other rare-earth oxides)	55.5	125.9	181.4
	1/4-in.	B_4C	75.2	128.8	204.0
	1/4-in.	Excess B_4C over R.E.	19.7	2.9	22.6
Open, poisoned	1/4-in.	B_4C	54.8	109.3	164.1
	1/4-in.	R.E.	40.7	107.9	148.6
	1/8-in.	90% Gd_2O_3	27.6	105.3	132.9
	1/8-in.	45% Gd_2O_3, 45% Sm_2O_3	34.2	106.3	140.5
	1/8-in.	45% Gd_2O_3, 45% Sm_2O_3 (at top edge of core)	9.1	35.4	14.5

E. FLUX DISTRIBUTION

1. Gross Axial and Radial Distribution

Overall distributions of the gross thermal flux were determined in various lattices and control-rod configurations by means of the cadmium difference method. Round "alindium" foils (75% indium, 25% aluminum), 5 mils thick x 1/2-in. diameter,

were placed in 20 mil-thick boxes of aluminum or cadmium. The axial exposures were taken by placing the boxed foils in a special graphite foil holder, or in milled cups on the side of fuel elements or poison holders; the center-to-center foil separation was 10 cm and the foil plane was vertical. Radial traverses were made at the midplane of the core in a series of vertical graphite plugs in which the foil planes were horizontal; or, with the abovementioned graphite foil holder in a series of radial locations. The foil activations were counted on scintillation counters using automatic decay correction. Other corrections were applied to the data for background, foil normalization, resolving-time losses, and in the case of radial traverses, for cell location and relationship to the estimated local core boundary.

Figures 12 and 13 show the radial and axial flux distributions for the 22-element open lattice with a poison column of five rare-earth slugs inserted in the central lattice location. Figures 14 and 15 show the radial and axial distributions for the 30-element open poisoned-core-and-reflector lattice. Note the skewed shape of the total axial flux in Figure 15, due to the partial insertion of rod No. 4, with its axis located 21 inches from the axis of flux observation. This traverse

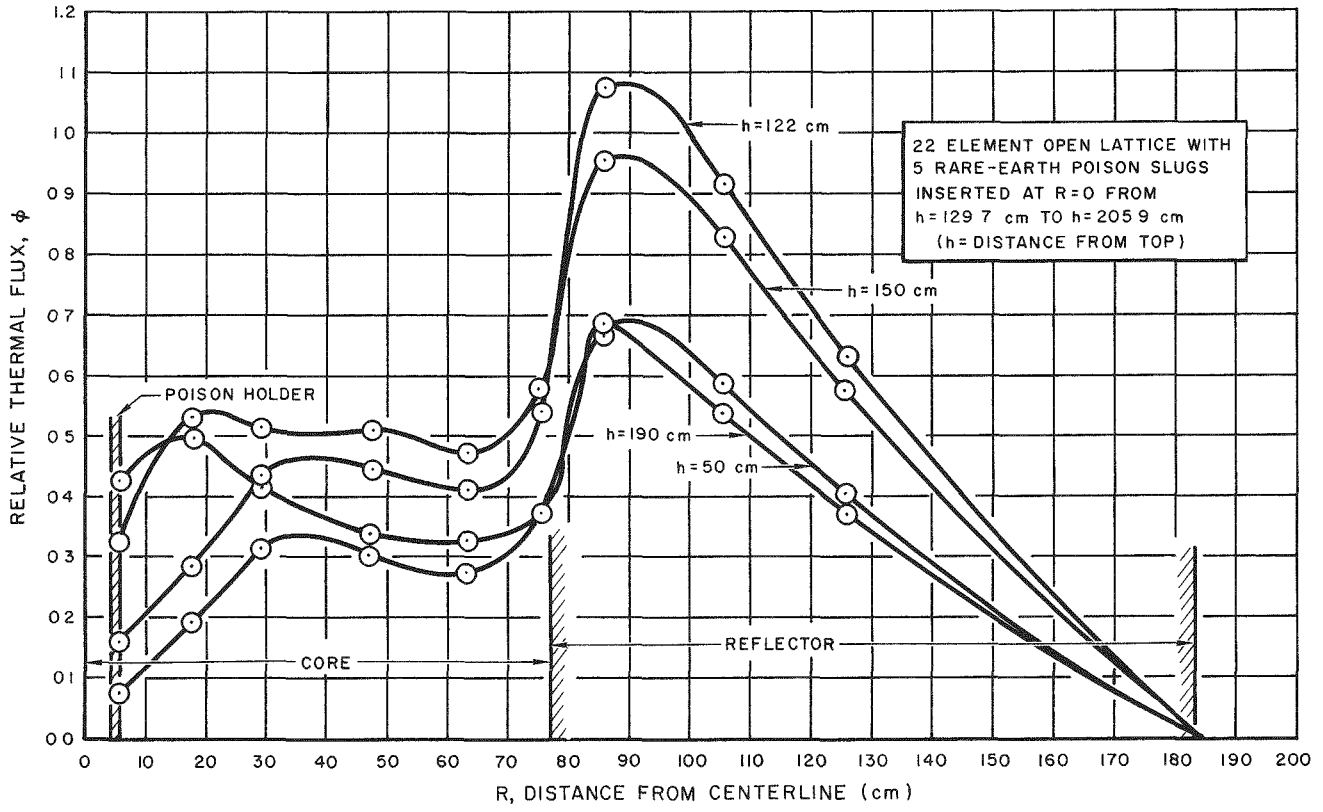

Figure 12. Radial Thermal Flux Distribution

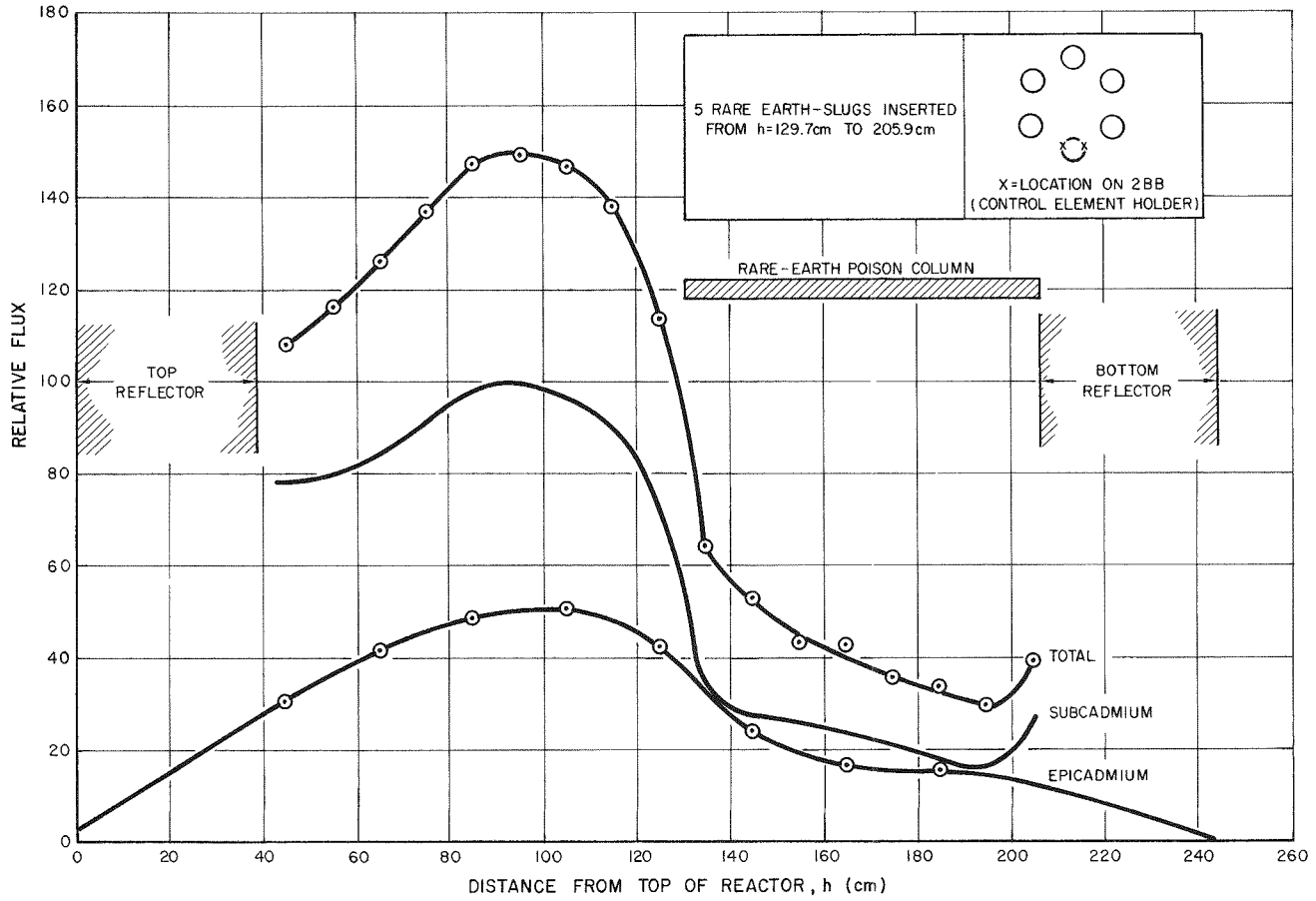

Figure 13. Axial Flux, Traverse Along Poison Holder

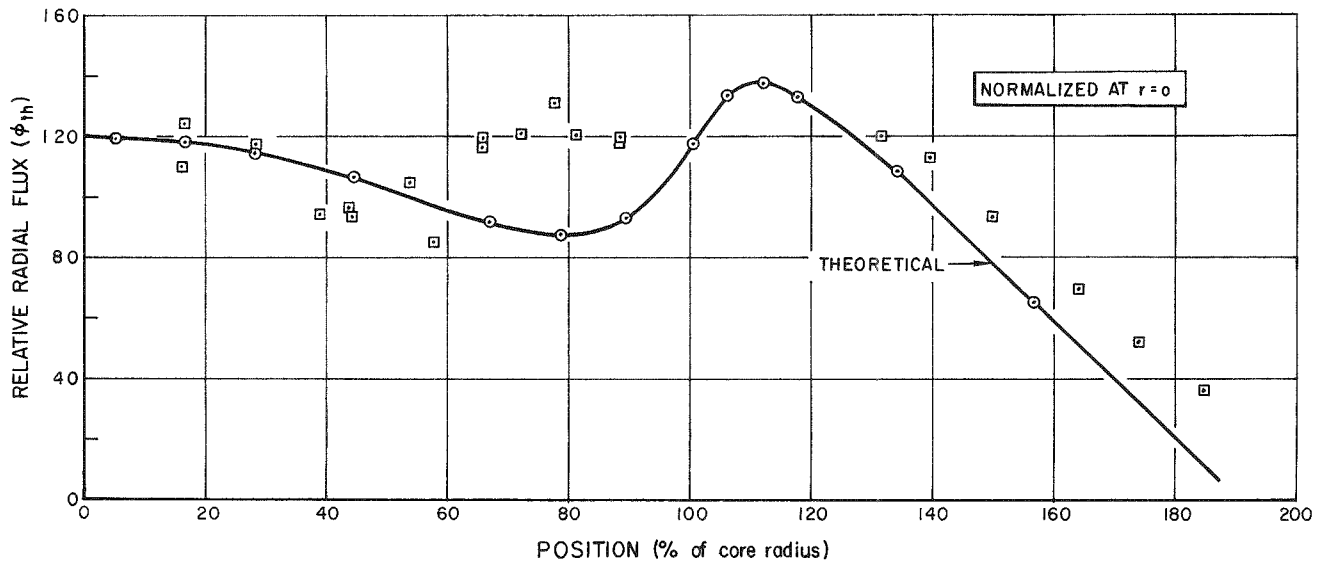

Figure 14. Radial Flux, 30-Element Lattice

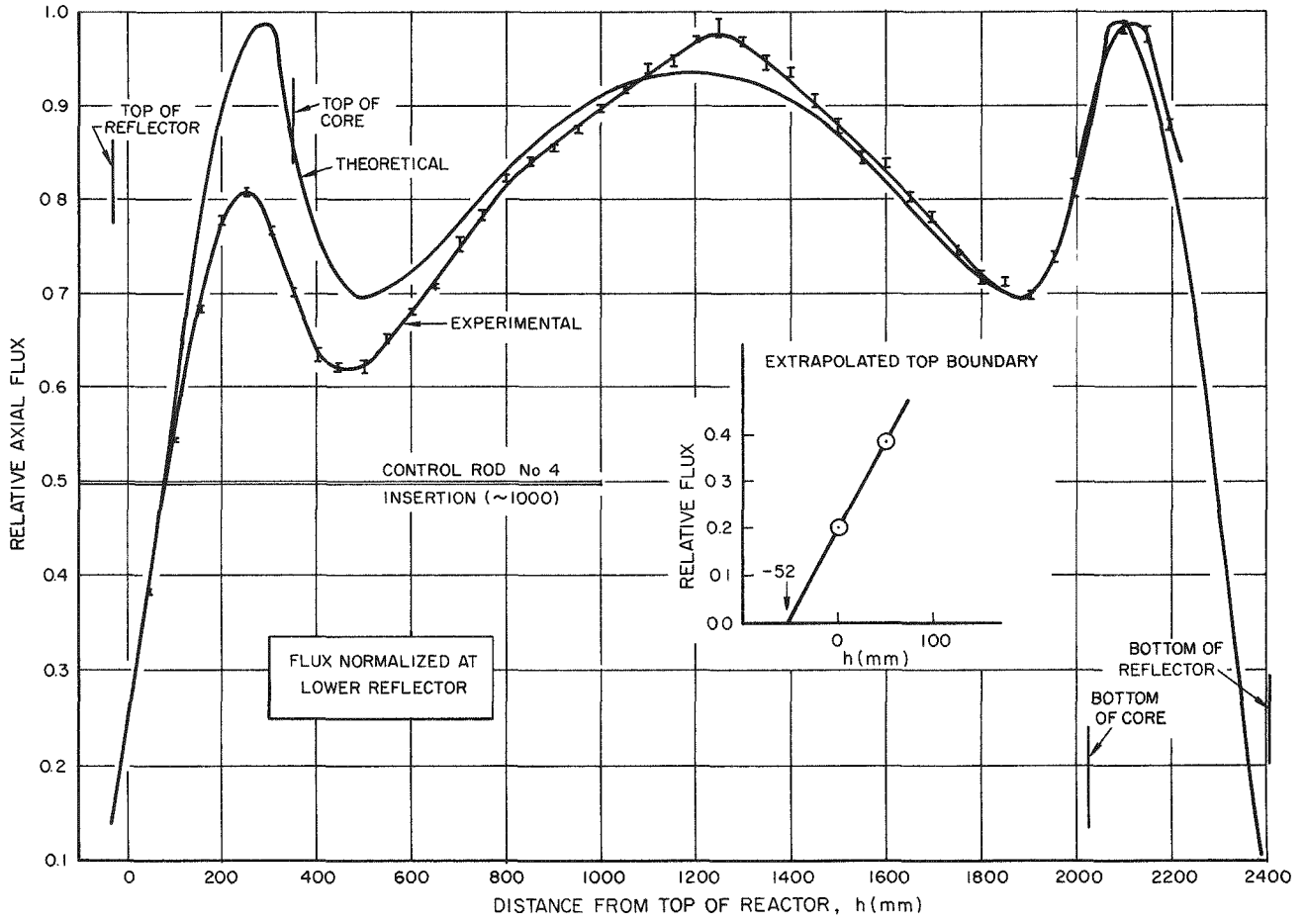

Figure 15. Axial Flux, 30-Element Lattice

was taken with a miniature fission counter, about 1/4-in. in diameter, which was attached to a drive mechanism similar to that of a control rod. The counter traveled in a slot milled into the side of a 2-in.-diameter graphite plug extending axially through the reactor. The power level was held constant (within 1%) throughout the traverse. The effective axial location of the fission counter was determined by extrapolation of the data to zero and the assumption of a 2-cm extrapolation length.

2. Perturbation of Power Distribution (About a Partially Inserted HNPF Control Rod)

A series of axial flux traverses were made, with the same foils as above, about a partially inserted Hallam control column (five rare-earth slugs in the poison holder). These traverses were made at various locations throughout one of the hexagonal cells which intersect the poison site, and at 60° separations on

the surface of a neighboring fuel element (all three nearest neighbors were located symmetrically with respect to the test element). These data have been used to determine the perturbation of the power distribution in the lattice due to the partial insertion of a control rod.

The azimuthally averaged surface fluxes can be used to represent the axial power distribution throughout the fuel volume of a nearest-neighbor element (Figure 16). The fluxes around the next closest ring of fuel elements show only a slight skew from the normal distribution, so that a normal power distribution holds for all but the first-ring elements.

F. THERMAL UTILIZATION (With stainless steel tubes)

As mentioned earlier, stainless steel tubes were used to poison the lattices and significantly increase the core diameter. The volume of steel introduced was computed in the following manner to approximate the neutron absorption rate of the various cladding and structural materials present in the HNPF lattices. The flux distribution in a cell was assumed to be given by the intracell data obtained in the exponential experiments on the 16-inch full lattice; then, the results of other exponential experiments, in which steel was placed around the

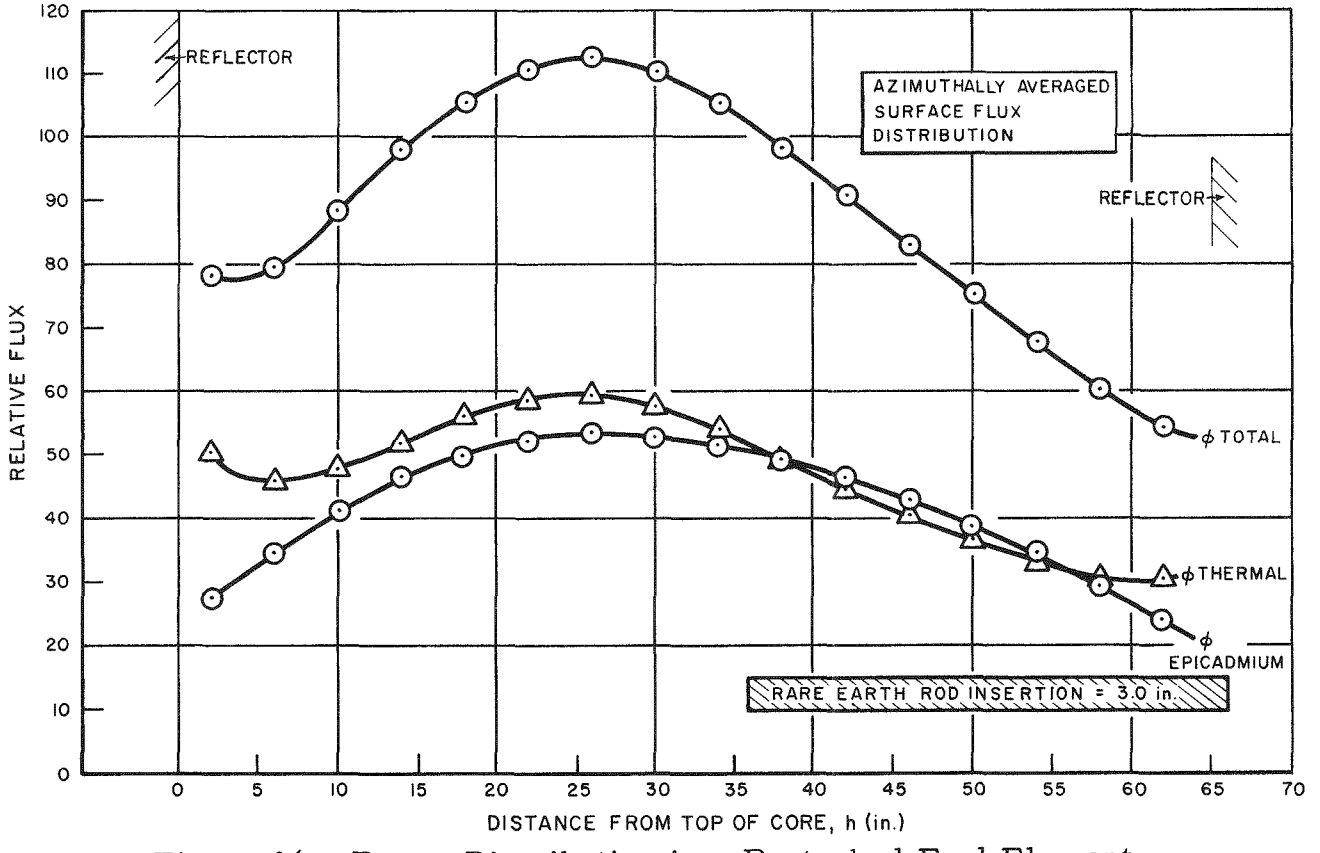

Figure 16. Power Distribution in a Perturbed Fuel Element

graphite logs and fuel element of one cell to simulate the HNPF poison geometry, were used to provide a value of the stainless-steel thermal utilization. This value was then used to determine the volume of stainless steel tube required at the center of each hexagon to provide the same ratio of poison absorptions in the critical lattice. This procedure gave a required volume of 0.3747 in.^{2}/hex = 0.1874 in.^{2}/cell, but neglected the depression of the flux by the tube, and differences in graphite grades; (the exponential experiments used graphite similar to that of the HNPF).

A determination of the actual effect of the stainless steel tubes on the critical-experiment lattices was performed. Foil exposures were made at the midplane of the core with and without an SS tube in the hex, to determine the approximate change in thermal utilization. This gave the following ratios of average fluxes in the poison tube, graphite, and fuel element surface:

$$\overline{\phi}(\text{SS})/\overline{\phi} \text{ (at outer aluminum surface)} = 1.66,$$

and

$$\overline{\phi} \text{ graphite (with SS)}/\overline{\phi} \text{ graphite (without SS)} \approx 0.90 .$$

Though this last value is very approximate because of the incomplete coverage of the graphite in the traverse, it has only a small effect on f for the lattice. By using these values, together with a value of f from an Sn calculation for open lattices, the following change in thermal utilization due to the poison addition was found:

$$f \text{ (fuel)} \simeq 0.893 \text{ in the unpoisoned open lattice (calculated)}$$

and

$$f \text{ (fuel)} \simeq 0.854 \pm 0.004 \text{ in the open poisoned lattice.}$$

The value of $\Delta k/k = \Delta f/f = 4.37 \pm 0.45\%$ obtained from these values agrees quite well with the observed reactivity change resulting from poisoning the lattice as

determined from summation of the worths of the additional fuel elements necessary for criticality in the open poisoned lattice; i.e.,

$$\frac{\Delta k}{k} = \sum_{i=17}^{25} \rho_i + \rho \text{ excess(16 element core)} - \rho \text{ excess(25 element core)}$$

$$= \$6.72 = 4.70\%$$

where ρ_i = denotes worth of i th element.

A reactivity worth measurement on a stainless steel tube in a near-center location (distance from center plug = 9.24 in.) in the 29-element lattice gave ρ_{ss} = - 72.3 cents, which is also in reasonable agreement with the above results.

IV. CALCULATIONS

A. METHODS USED

The cell fluxes and the flux- and volume-weighted thermal Maxwellian microscopic cross sections of the core were computed[6] with the S_4 cell code on an IBM-709 computer, using the material cross sections in Table VIII. Three-fast-group cross sections were obtained[7] for the core and reflector regions with the MUFT-IV code, using homogenized material densities. Finally, AIM-5, a multigroup, one-dimensional, diffusion-theory code, was employed, using four energy groups, to calculate the critical loadings, material bucklings, and flux and adjoint distributions for the various lattices[8].

TABLE VIII

SUMMARY OF MATERIAL DATA

Material	Type	Density (g/cm^3)	Wt/Element (kg)	$(1-\bar{\mu}_o)\,\sigma_s$ (barns)	$\bar{\sigma}_a$ max (T = 20°C) (barns)
Graphite	AGOT	1.68	-	4.534	4.38×10^{-3}
Aluminum	1100	2.7	-	1.365	0.195
Fuel (U-Mo)	-	17.12 ± .02	-	-	-
U^{235}	3.448 at.%E	0.530	2.834	9.972	600
U^{238}	-	14.85	97.200	8.27	2.48
Mo	10.15 wt%	1.738	-	6.952	2.4
Fuel-UC	-	13.2	-	-	-
U^{235}	3.448 at.% E	0.427	2.609	See Above	
U^{238}	-	12.12	-	See Above	
C	4.95 wt%	0.625	-	See Above	
Stainless Steel	304	7.87	-	9.7	2.62

Cylindrical geometry was imposed on the S_n cell calculations, which necessitated several simplifying geometrical assumptions to make a cell model which could be described within the code geometry. A description of the cell models adopted for each of the various lattices is given in the next section.

Volume-weighted number densities for the MUFT-IV code were computed from the cell geometry (Figure 5), the lattice geometry, and the material data listed in Table VIII.

Self-shielding factors, L, must be entered in the MUFT-IV code for all lumped resonance absorbers; a rubber-band surface was chosen to depict the effective fuel surface of the 18-rod cluster, and an L-factor was computed from this to give the resonance integral in U^{238} in accordance with Hellstrand's[9] formula for uranium metal. A modified-Dancoff correction[10] of 15% was applied to the rubber-band surface in this formula to account for the inner fuel surfaces which are supplied with aluminum-moderated resonance-energy neutrons. The effective resonance integral for molybdenum gives the best fit between calculated bucklings[11] and bucklings measured in the exponential experiments[1] when set equal to 5 barns; therefore, the Mo L-factor was chosen to give this value in the MUFT-IV code. The 5-b value also may be deduced directly from recent measurements of 21 to 22 b for the infinitely dilute molybdenum resonance integral carried out at Harwell[12] and UCRL,[13] and from the use of molybdenum resonance parameters.[14]

The bucklings used in both the MUFT-IV and AIM calculations were assumed to be constant over all spatial regions and energy groups.

B. CASES STUDIED: CELL MODELS

For the thermal core-averaged properties, it was necessary to perform calculations on a small repeating portion (cell) of the core by use of transport equations (S_n code). This code permits solving for the flux distribution in the cell and computation of effective flux- and volume-weighted cross sections of the cell; hence, of the core. For the more complex lattices, it was necessary first to compute individual portions of the cell (subcells), and then to use these results in a final cell (supercell) calculation to obtain the thermal core properties. This method was used in lieu of a single two-dimensional calculation.

For the full lattice, a single cell was used, which consisted of one fuel element surrounded by a cylindrical graphite region; the total cell area equals half the area of one hexagon (16-in. across flats) of the core pattern. The fuel element was subdivided into six cylindrical regions: a central void, aluminum, Al + fuel, Al, Al + fuel, and Al. Material properties were volume-weighted in those regions where necessary, in order to obtain homogeneous cross sections for each

region. The results of this calculation give the thermal core properties for the full lattice. This model of the fuel element was also used in all of the following cell calculations.

Because of the complexity introduced in the open lattice by the vacancies at every sixth lattice site, it was necessary for this case to use a supercell consisting of six lattice sites, with a total area of three times the area of a 16-in. hexagon. This supercell was then pictured as consisting of two types of subcells: five fuel-and-graphite cells, as described above, and one graphite cell with a void in the central region, each cell having 1/6th the area of the supercell. An S_n calculation was run, in which the graphite-and-void cell is surrounded by five fuel cells in the shape of a cylindrical region, to obtain cell-averaged thermal core properties for the open lattice. Neutron streaming was not accounted for by this method.

The open poisoned lattice introduces one more complexity; therefore, one more subcell was needed, which consisted of a central graphite region, the stainless steel annulus, and an outer graphite region. The 4-in. radius of this subcell was chosen to have the outer cell boundary near the point of maximum flux in the composite cell, since the condition $\partial \phi / \partial r = 0$ is imposed at the outer boundary in a cell calculation. The areas of the first region and of the fuel subcells were reduced to make up for the cell area taken up by the stainless steel subcells; a cell calculation was then run on this small fuel cell. The supercell was then composed of a small graphite subcell surrounded by an annulus of three stainless steel subcells, whose properties were obtained as described above, and a third region of five small fuel cells. Vacant lattice sites were here assumed to be plugged with graphite.

For the poisoned-reflector case, the outer region of the above model of the supercell was assumed to be graphite; the resultant S_n-determined properties were then ascribed to an equivalent poison-reflector region and were used in the AIM calculations for the poisoned-core-and-reflector open lattice.

The supercell of the full poisoned lattice used the same subcells and region volumes as that of the open poison lattice, except that the central region had the same material properties as did the outer region.

C. RESULTS AND COMPARISONS

1. Buckling

Material bucklings of the various lattices were computed by running axial bare-core AIM calculations with transverse-buckling criticality searches. From these values and the results from axially reflected runs, the axial reflector savings and axial buckling values were determined. The latter were used in the radially reflected one-dimensional criticality searches, which determined the critical core radius of the fully reflected reactor. From this data and from the radial buckling found above, the radial reflector savings can be determined. A summary of the calculated values of material bucklings and reflector savings is given in Table IX. A comparison with bucklings measured on the exponential assembly (using HNPF-grade graphite) is also shown.

TABLE IX

CALCULATED REFLECTOR SAVINGS AND MATERIAL BUCKLINGS

Lattice	B_m^2 (m^{-2})	δ_{ax} (cm)	δ_{rad} (cm)	B_m^2 (exponential[1]) (m^{-2})
Open	6.30	40.1	55.0	5.46*†
Full	5.70	37.1	55.8	5.50 ± 0.07†§
Open, poisoned	4.98	35.5	54.3	-
Open, poisoned core and reflector	4.98	35.5	48.5	-
Full, poisoned	5.27	37.1	56.8	-

*No error limits appear on this value, although the experimental error is of the same order of magnitude as that given for the full lattice value, because of the large streaming effect of the voided vacant lattice site, for which correction was not made.

†The graphite used in the exponential experiments has a $\Sigma_a = 0.00059$; for comparison with the calculated values, these results should be increased by approximately 0.30 m^{-2}.

§The fact that little or no change in buckling is observed by filling the void locations with fuel elements is in line with the results of Section III-B.

2. Critical Mass

The critical number of cells can be computed from the critical core area divided by the cell area. A compilation of the calculational results, and a

comparison with the experimental critical sizes, is given in Table X. No attempt has been made to adjust the various parameters of the calculations to achieve results closer to the experimental values as yet; however, this may be done at a later date.

TABLE X

CALCULATED AND MEASURED CRITICAL MASSES

Lattice	Critical No. of Fuel Elements	No. of Dummy* Cells	Total Cells (Experimental)	Calculated Cells
Open	15.1	1	(16.1)†	13.6
Full	17.0	-	17.0	17.8
Open, poisoned core	22.4	2	24.4	27.0
Open, poisoned core and reflector	27.6	4	31.6	31.2
Full, poisoned core	25.2	-	25.2	21.7

Note: All calculations assumed an effective molybdenum resonance integral of 5 b and a S of 15% on the U^{238} rubber-band surface. Further, all experiments and calculations were with all void locations (if any) plugged with graphite.

*Because of the small critical core size and the fact that a vacancy was chosen to be at the center of the lattices, many of the prescribed void locations were outside the core boundaries and sensibly no different from the reflector. Thus, the number of cells in the core was not increased by the expected ratio of 6/5 times the number of fuel elements for the open lattices.

†In this extreme case, what was actually measured, was a full lattice without a central element; all other vacant lattice sites are out of the core.

3. Element Worth

The iteration steps of the AIM program,which are printed out along with the final result, can be used to determine the peripheral worth of a small ring of core area, which can be related to number-of-cells by the cell area. In this manner, the peripheral fuel element worth in the open poisoned core and reflector lattice was calculated to be 47¢, compared with an experimental worth of 65¢. For the full poisoned lattice, these numbers are 63¢ and 57¢ respectively.

4. Fluxes

Theoretical fluxes were also computed by the AIM-5 code. A typical four-group flux distribution is shown for the poisoned open lattice in Figure 17. A comparison is made between calculated and experimental thermal fluxes in Figure 16 (See section III-E) with the two magnitudes normalized at the unperturbed reflector (in the experiment, rod No. 4 is partially inserted and perturbs the flux in the upper portion of the curve).

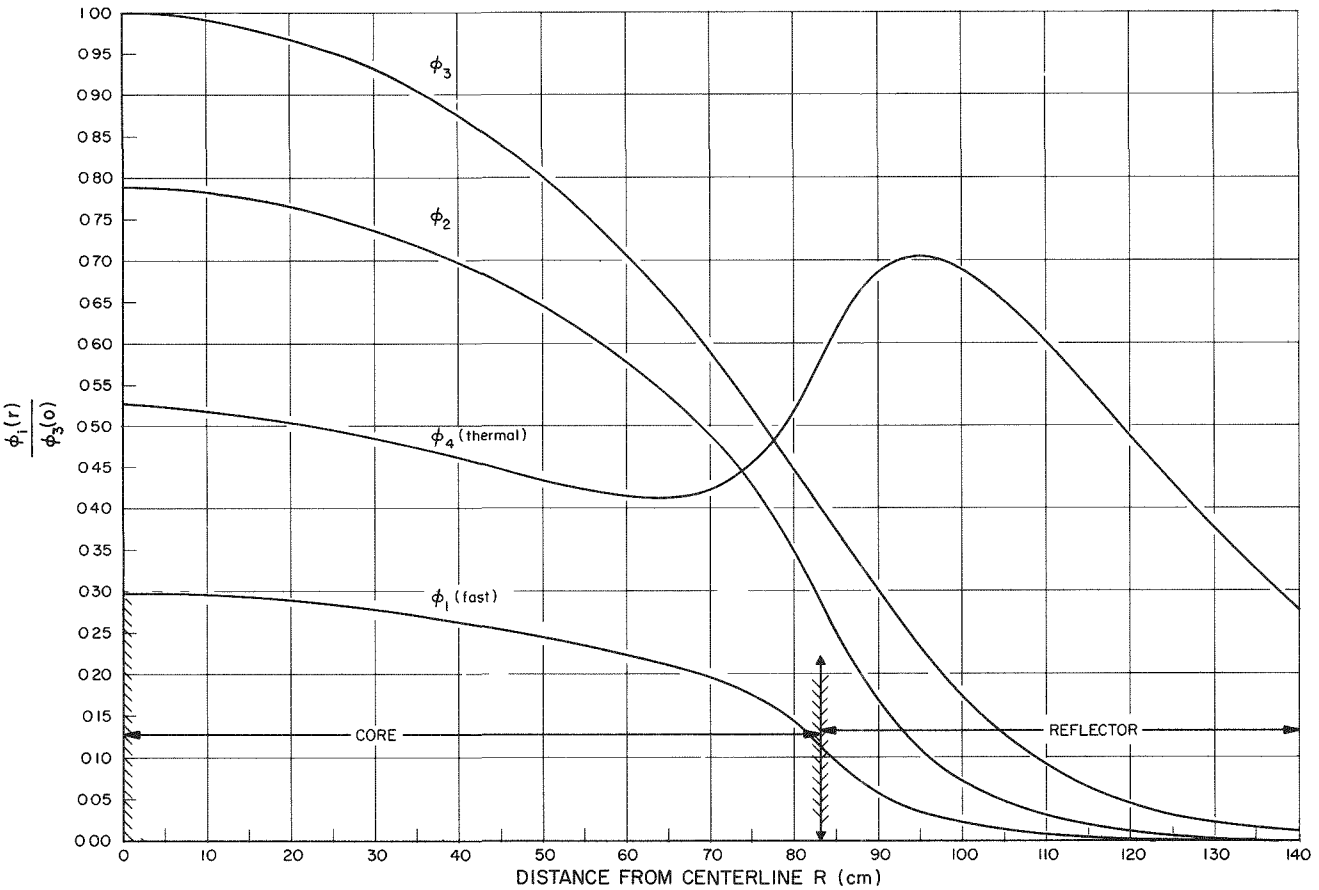

Figure 17. Calculated Radial Fluxes in Open, Poisoned Lattice

REFERENCES

1. O. R. Hillig, "Exponential Experiments for the Hallam Nuclear Power Facility," (to be published)

2. F. Gronemeyer, "75,000 Watts of Electricity by Nuclear Fission at the Hallam Nuclear Power Facility," AI-5272 (June 1960)

3. D. E. Fletchall et al., "Sodium Graphite Reactor Critical Experiment Hazards Summary," NAA-SR-3404 (April 27, 1959)

4. Private communication, K. E. Buttrey

5. L. S. Beller, "An Accurate Reactivity Measurement Technique for Critical Facilities," in Trans. Am. Nucl. Soc. 3-1, 77 (1960)

6. J. H. Warner and H. P. Flatt, "S_4 and S_8 Cylindrical, and S_4 Plane Geometry Cell, N Regions Calculations," NAA Program Description (September 1959)

7. J. Bohl et al., "MUFT-IV, Fast Neutron Specturm Code for the IBM-704," WAPD-TM-72 (July 1959)

8. H. P. Flatt and D. C. Baller "AIM-5 Diffusion Equation Codes," NAA Program Description (September 17, 1959)

9. E. Hellstrand, J. Appl. Phys., 28, 1493 (1957)

10. E. Critoph and A. G. Ward, "Comparison of Theory and Experiment for (A) Lattice Properties of D_2O-U Reactors, (B) Central Rod Experiments (C) Foreign Rod Experimpent," CRRP 655 (July 26, 1956)

11. M. Aronchick, "Nuclear Characteristics of the Hallam Mark B Core," NAA-TDR-5305 (July 20, 1960)

12. R. B. Tattersall, et al., "Pile Oscillator Measurements of Resonance Absorption Integrals," AERE-R 2887 (1959)

13. E. Goldberg, "Resonance Absorption of Neutrons in Molybdenum," UCID-4131 (January 18, 1960)

14. D. J. Hughes and J. A. Harvey, BNL 325, Second Edition (July 1958)